Monitoring the Allosteric Transition and CO Rebinding in Hemoglobin with Time-Resolved FTIR Spectroscopy†

Ruopian Chen and Thomas G. Spiro*

Department of Chemistry, Princeton University, Princeton, New Jersey 08544

Received: July 2, 2001; In Final Form: October 23, 2001

Time-resolved FTIR spectra are reported for the photocycle of carbonmonoxy hemoglobin, under saturating photolysis conditions, which are sufficient to drive the R−T allosteric transition. Direct evidence for this transition was provided by the microsecond time scale evolution of an 1857 cm^{-1} bisignate difference band (cysteine S−H stretching), which is a marker of the T state. The time course of the strong 1951 cm^{-1} band of bound CO showed the expected fast geminate and slower second-order rebinding phases. Two slow phases were observed, having time constants consistent with reported binding rates for R and T state molecules. The geminate yield was 50%, the majority (37%) rebinding with a 70 ns time constant, consistent with previous studies, but an additional low-amplitude (13%) phase was resolved, with an 890 ns time-constant. Difference FTIR bands are also observed in the 1300−1700 cm^{-1} region, where protein vibrations are expected. In the nanosecond regime these bands varied irregularly, due to instrument limitations, but in the microsecond regime they evolved (30 μs time constant) toward the static difference spectrum of HbCO minus deoxyHb, reflecting the expected evolution from R to T state photoproduct molecules. The difference spectra of R and T photoproduct molecules extracted from the data via kinetic analysis contain not only common bands but also bands that are distinctive. The R photoproduct difference spectrum contains a positive/negative band pair at 1649 and 1683 cm^{-1}, which is interpreted as resulting from the breaking of one or more α-helical carbonyl H-bonds. Candidate H-bonds are those that connect the H-helix residues Tyr α140 and β145 with the F-helix residues Val α93 and β95, in both HbCO and deoxyHb. These H-bonds are believed to break and reform at intermediate stages of the allosteric pathway, on the basis of UV Raman evidence.

Introduction

We report the first kinetic analysis of the R−T transition in hemoglobin using time-resolved infrared spectroscopy. Intermediates in the allosteric pathway of Hb have previously been identified by analysis of time-resolved absorption[1] and resonance Raman[2] spectra obtained after photolysis of the CO adduct (HbCO). The resonance Raman spectra of the intermediates identify structural changes at the heme and at tyrosine and tryptophan residues of the protein. A working model of the allosteric reaction coordinate has been proposed on the basis of these changes.[2,3]

Infrared and Raman spectroscopy are complementary techniques for monitoring molecular vibrations. Raman spectroscopy has the advantage that tuning the laser excitation wavelength to selective transitions enhances the scattering from vibrations of chromophoric molecular groups; the resonance Raman effect provides both selectivity and molecular sensitivity. The disadvantage is that nonchromophoric regions of the molecule may escape detection. The IR spectrum, on the other hand, is nonselective and captures all molecular vibrations (except those forbidden by symmetry, a condition not found in proteins.) Its disadvantages are low molar intensities and spectral congestion. However, some molecular vibrations stand out in the IR spectrum and are useful markers.

IR studies of proteins have focused largely on carbonyl stretching vibrations of amide groups and of carboxylic acid side chains, which generate large dipole changes and strong IR bands. Time-resolved FTIR spectroscopy can extend the power of IR analysis by producing high-precision difference spectra associated with structural changes.[4] Application to the HbCO photocycle can provide additional structural probes of the allosteric intermediates. In a previous study, Hu et al. reported step-scan FTIR spectra of the HbCO photocycle on the nanosecond and microsecond time scales.[5] The time course of CO rebinding was accurately determined, and fast dynamical behavior was observed for several protein difference bands. However, the degree of photolysis achieved in the experiment was insufficient to drive the R−T transition. Thus, the observations were limited to tertiary changes within the R quaternary structure. In the present study we increased the light intensity sufficiently to achieve essentially complete photolysis and were able to observe evolution of the T quaternary structure as monitored by a cysteine S−H marker band. Many protein difference bands changed markedly during the evolution. On the basis of their dynamical behaviors, it is possible to associate these bands with the R or the T quaternary structures. Some tentative assignments to protein residues are suggested. In addition, the time course of CO recombination reveals a previously undetected geminate phase, with a 0.9 μs time constant and an amplitude corresponding to 13% of the geminate rebinding. This phase is attributed to CO molecules, which escape the heme pocket but rebind from other locations within the protein.

Experimental Section

Sample Preparation. Adult human hemoglobin (HbA) was prepared from fresh human blood by standard procedures.[6] The

† Part of the special issue "Mitsuo Tasumi Festschrift".

10.1021/jp012491v CCC: $22.00
Published on Web 01/09/2002

purified samples were diluted in D_2O buffer saturated with carbonmonoxide gas and then reconcentrated. The procedure was repeated three or four times to ensure that exchange of H_2O by D_2O was more than 98%, as judged by the IR absorption of water at 3400 cm^{-1}. The deuterated sample was left in the D_2O buffer for at least 36 h to allow complete exchange of labile protons. The final concentration of HbA was about 2 mM (in heme) in 50 mM phosphate buffer at pD = 7.4 saturated with 1 atm of CO gas.

Spectral Measurements. A Bruker IFS 88 FTIR spectrometer with a step-scan option was used in this project. The step-scan FTIR instrumentation was described previously.[5] A low-pass filter was used to limit optical throughput and avoid aliasing. For static FTIR spectra obtained in rapid-scan mode, double-sided interferograms were collected to ensure proper phase correction. The Mertz phase correction algorithm was utilized with 256 data points taken before and after the zero retardation point. Spectra were collected at 4 cm^{-1} spectral resolution. Data analysis was carried out with the OPUS software from Bruker Optics and the Grams software package (Galactic Industries).

CaF_2 windows are used to give unobstructed access to the spectral window above 1200 cm^{-1}. Their transparency in the visible region also permits the acquisition of visible absorption spectra of the loaded FTIR cell taken before and after infrared measurement to check sample integrity (absence of metHb). A cell spacer of 50 μm thickness (Teflon, Spectra Tech) was used for the D_2O solutions. This short path length kept the absorption of the most intense band in the spectrum below 0.9 absorbance unit, thereby ensuring linear operation of the IR detector. The actual path length was calculated from the interference fringe pattern of the empty cell. The temperature of the sample was kept at 22 $\pm$ 1 °C during the experiments. Heating effects are minimal because of good thermal conduction to the windows of the IR cell; no protein degradation was detected even after 5 h of irradiation. The FTIR spectra were collected in blocks of 100−400 scans. Block co-addition of scans ensures that systematic errors cancel and that artifacts due to sample deterioration do not accumulate. The number of co-added spectra ranged from 1000 to 4000 scans, depending on the SNR requirement of the spectral features of interest.[7]

Time-resolved spectra were measured in step-scan mode. In the nanosecond regime, a 50 MHz photovoltaic MCT detector (Kolmar Technology) with a built-in low-noise preamplifier was employed. The liquid nitrogen cooled MCT infrared detector can cover the entire spectral region of interest with high sensitivity. The built-in preamplifier provides two outputs: a DC output furnishing the static interferogram and an AC output furnishing the laser-induced change of the interferogram. The AC-coupled signal was amplified by a factor of 125, and DC-coupled signal was amplified by a factor of 5 by another amplifier (500 MHz), in order to make use of the full dynamic range of an 8-bit digitizer (200 MHz). Both AC- and DC-coupled signals were then simultaneously sampled, and Fourier transformation of the AC-coupled interferogram was implemented with the phase obtained from the DC-coupled interferogram.

The time response of the system was ~25 ns, as determined via the scattered 1064 nm radiation of the ~9 ns laser pulse of a Nd:YAG laser.[4c] The signal was taken directly from the detector to the fast digitizer (100 MHz), which was triggered and synchronized by part of the same pulse. In the frequency domain, the spectrum shows only one sharp peak at 9398 cm^{-1}, the exact wavelength of the 1064 nm radiation. The 9398 cm^{-1} band has a nearly symmetric time response with a full width at half maximum of 40 ns, showing that the time-resolution of the system is about 25 ns. Transient difference FTIR spectra from 10 to 4000 ns were recorded at 10 ns intervals. One-sided interferograms with 570 mirror positions were collected to obtain 4 cm^{-1} spectral resolution with a spectral window of 2050−1120 cm^{-1}. At each mirror position 60 signals were averaged in order to increase the signal/noise ratio, resulting in a total data collection time of around 1 h per experiment. Data from 20 successive 1-h scans were averaged for further signal/noise improvement.

The second harmonic emission (532 nm) of a Q-switched Nd:YAG laser (~9 ns pulse width, 10 Hz) was used as the pump laser. Power dependence experiments were carried out to determine the required power level for full photolysis. The CO absorption difference in the HbCO FTIR spectra saturated when the laser power reached ~21 mJ per pulse on a ~7 mm spot. This was the power level used for the time-resolved FTIR experiments.

The microsecond time-resolved measurements were performed similarly. A 200 kHz 16 bit digitizer was used, and a DC-coupled step-scan run was conducted first without excitation of the sample. The phase was stored and then used for Fourier transformation of the AC-coupled interferograms. The transient difference FTIR spectra from 5 μs to 1.5 ms were recorded at 5 μs intervals. Difference spectra (ΔA) were calculated as described by Uhmann et al.[8]

Since the measured time response of the detector was ~25 ns (vide infra), three 10-ns time slices were co-added and taken as single data points for kinetic analysis of the CO stretching bands in the nanosecond regime. In the microsecond time regime, however, no co-addition was necessary.

Results

Nanosecond Regime. Difference FTIR spectra between unphotolyzed HbCO and its photoproduct in the nanosecond regime [Figure 1] reveal decreasing difference intensity of the strong 1951 cm^{-1} FeC−O stretching band, as expected for geminate recombination. The time course of CO recombination [Figure 2] was determined by determining the ratio of the 1951 cm^{-1} intensity of the photoproduct to that of unphotolyzed HbCO. Two exponentials are required to fit the data, with time constants of 70 $\pm$ 15 and 890 $\pm$ 90 ns. The amplitudes of these two phases represent 33% and 12%, respectively, of the full HbCO intensity. The fitted curve was extrapolated to 10% of the HbCO intensity at zero time. Since the laser power was set at a saturating value (see Experimental Section) the residual 10% of unphotolyzed HbCO is attributable to photoselection by the (polarized) laser pulse, as described by Eaton and co-workers.[9] Dividing the sum of the recombination amplitudes (45%) by 0.9 (the degree of photolysis) gives a geminate yield of 50%, in excellent agreement with estimates from absorption[1] and RR[2] transients. This 50% is divided between a 37% contribution from the 70 ns phase and a 13% contribution from the 890 ns phase.

The 70 ns time constant is in satisfactory agreement with the 50 ns values obtained from absorption[1] and RR[2] transient experiments. Jones et al.[10] subsequently resolved the fast absorption phase into two overlapping phases, with time constants of 20 and 90 ns. The 20 ns phase is too fast to be resolved in our experiment. The slow, 890 ns geminate phase has not previously been reported, perhaps because its amplitude is low. We note that the time constant coincides with a protein relaxation phase determined from both absorption[1,10] and UVRR[2] spectra.

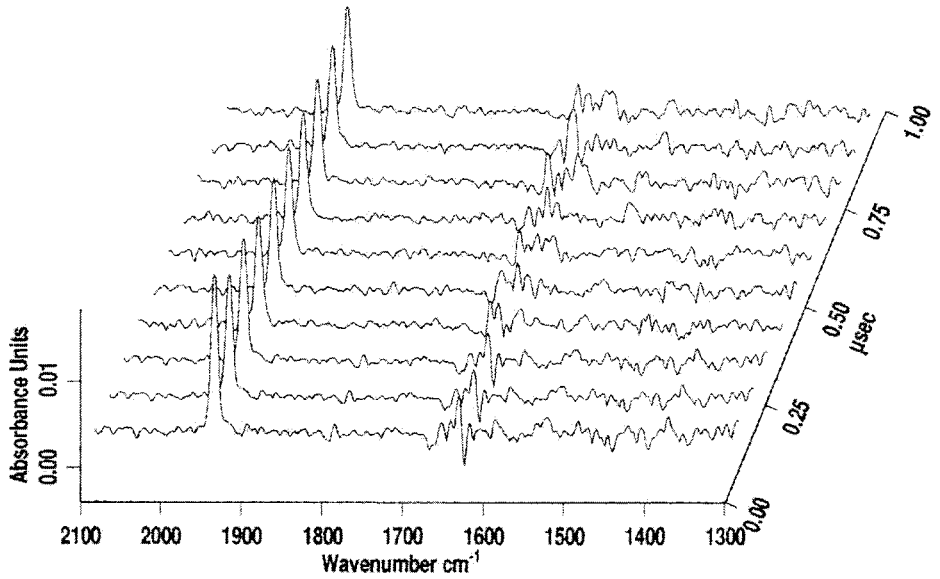

Figure 1. Evolution of HbCO-minus-photoproduct FTIR difference spectra in the nanosecond regime, showing decreasing difference intensity of the 1951 cm^{-1} CO stretching band due to geminate recombination. The features in the 1300−1700 cm^{-1} region vary irregularly with time and are attributed to noise.

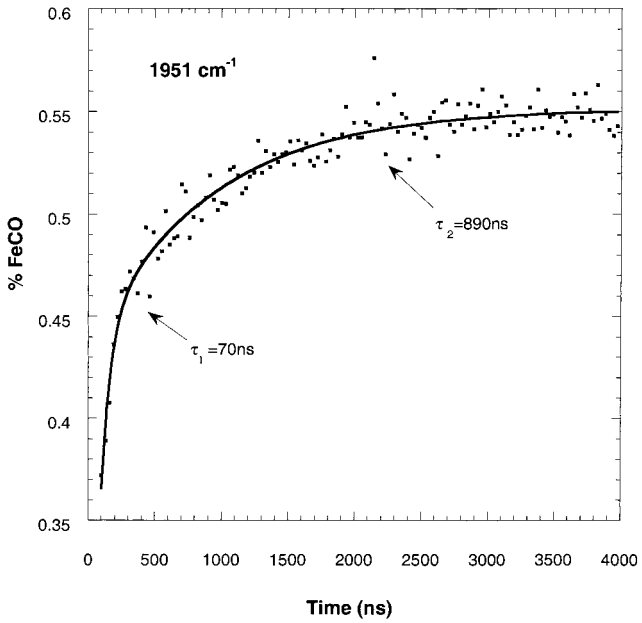

Figure 2. Amplitude of the 1951 cm^{-1} photoproduct band, as a fraction of the HbCO amplitude. The solid curve is a fit to the data with two successive exponentials, having the indicated time constants.

In addition to the 1951 cm^{-1} CO band, the difference spectra show features in the 1300−1700 cm^{-1} region, where protein IR bands are expected. However, these features vary in an irregular manner from one experiment to another, an effect attributed to electronic noise. The combination of high absorbance and small absorbance difference (and also short acquisition time) severely limits the signal/noise ratio in our experiment.

Microsecond Regime. At time delays greater than 5 μs, systematic changes are seen for difference bands in the protein region, as well as for the CO stretching difference band [Figure 3]. The CO recombination time course [Figure 4] can be fit to two successive exponentials with time constants of 80 ± 4 and 670 ± 12 μs. We identify these with CO rebinding from solution to R and T state molecules.[11] Mathews and Olson report second-order rate constants of 2.9 and 7.1 × 10^6 M^{-1} s^{-1} for CO binding to the α and β subunits of the R state and 0.12 and

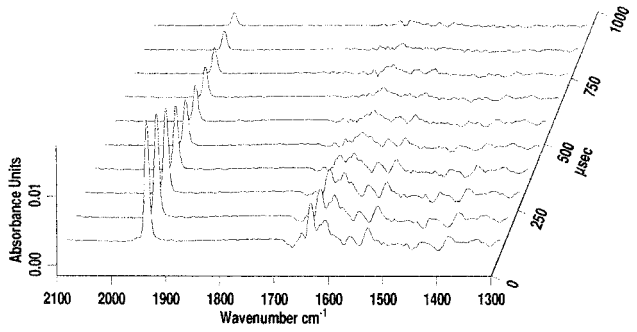

Figure 3. Evolution of HbCO-minus-photoproduct FTIR difference spectra in the microsecond region, showing decay of the difference intensity for the 1951 cm^{-1} CO stretching band, and of protein difference bands (1300−1700 cm^{-1}), accompanying CO rebinding.

0.18 × 10^6 M^{-1} s^{-1} in the T state.[12] At ambient CO concentrations (1 mM for CO saturated in water), these values translate to pseudo first-order time constants of ∼0.12 and ∼2.3 ms for R and T state molecules (average of α and β chains). At the high protein concentration in our experiment, pseudo-first-order conditions do not apply. However, a more elaborate fit to the data is not justified in view of the complexities of the system. The two exponentials fit the data to within experimental error.

When the protein difference bands are examined between 5 and 100 μs [Figure 5], a distinctive evolution is observed toward the spectrum expected for the T state (see HbCO minus deoxyHb difference spectrum[7] at the top). Particularly significant is the bisignate band at 1857 cm^{-1}, which arises from a shift[7,13] in the cysteine S−D stretching vibration that is characteristic of the T state. The signal is clearly observed at later (see inset) but not earlier times.

The microsecond evolution was further analyzed via kinetic traces of the difference FTIR signals. Two limiting behaviors were observed, as exemplified by the intensities at 1649 and 1677 cm^{-1} [Figure 6]. The 1649 cm^{-1} difference intensity decayed monotonically, with a time constant, 100 ± 3 μs, close to that of the fast recombination phase, attributed to CO binding by R state molecules. Thus the 1649 cm^{-1} band arises from the R state photoproduct, and has negligible contribution from the T state photoproduct. On the other hand, the 1677 cm^{-1}

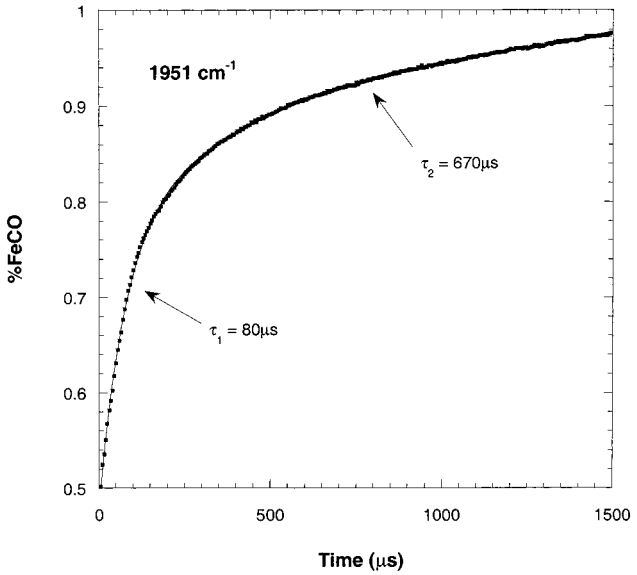

Figure 4. Amplitude of the 1951 cm^{-1} photoproduct band, as a fraction of the HbCO amplitude. The rebinding is modeled with two successive exponentials, with indicated time constants (although the rebinding is actually second order).

TABLE 1: HbCO-Minus-Photoproduct Difference Bands

R photoproduct (cm^{-1})	$(\Delta A)^{CO}$ %[a]	T photoproduct (cm^{-1})	$(\Delta A)^{CO}$ %[a]	tentative assignment
1951	51.7		43.4	
		1693	−1.4	amide I′
1683	−5.0			
		1676	2.0	
1666	4.0			
		1672	−2.0	
		1655	4.2	
1649	16.3			
1633	6.1	1632	5.4	
1622	8.5	1622	5.6	TyrY8a, TrpW1
		1611	4.4	
1591	−2.1	1591	−3.0	
1576	2.7	1579	4.3	COO^-, asym
1560	−2.1	1560	−2.1	amide II′
1545	6.6	1544	5.6	
1462	−2.4	1461	−3.4	
1444	0.8	1445	0.9	
1413	−2.6	1415	−3.2	
1395	3.4	1395	3.1	COO^-, sym
1345	1.5	1346	2.4	

[a] $(\Delta A)^{CO} = \Delta A/\Delta A_{HbCO} \times 100\%$. ΔA = difference FTIR absorbance at the indicated frequency, determined by peak area integration (Opus software, Bruker Optics). ΔA_{HbCO} = absorbance of the 1951 cm^{-1} band (0.0374) of unphotolyzed HbCO.

difference intensity initially increases from a value close to zero and subsequently decays. The rise time is 30 ± 5 μs while the decay time is 770 ± 100 μs, essentially the same as that of the slow CO recombination phase, attributed to T state molecules. Thus the 1677 cm^{-1} band arises from T state photoproduct. The rise time is 30 μs, in reasonable agreement with the ~20 μs transition seen in absorption[1,11] and UVRR[2] transients, which has been attributed to the R−T quaternary transition.

Intermediate behavior is seen for other FTIR difference bands. For example, the 1611 cm^{-1} intensity [Figure 6] rises with same time constant (30 μs) as the 1677 cm^{-1} band, but its decay rate (τ = 400 μs) is intermediate between the recombination rates for R and T photoproducts. Thus both R and T state photoproducts exhibit 1611 cm^{-1} difference bands, although the intensity is higher for the T photoproduct.

Using these FTIR time constants, we adopted a kinetic scheme in which CO recombined with R and T photoproducts with 80 and 670 μs time constants, respectively, and the R photoproduct converted to the T photoproduct with a 30 μs time constant. From the time variation of the concentrations, we extracted the

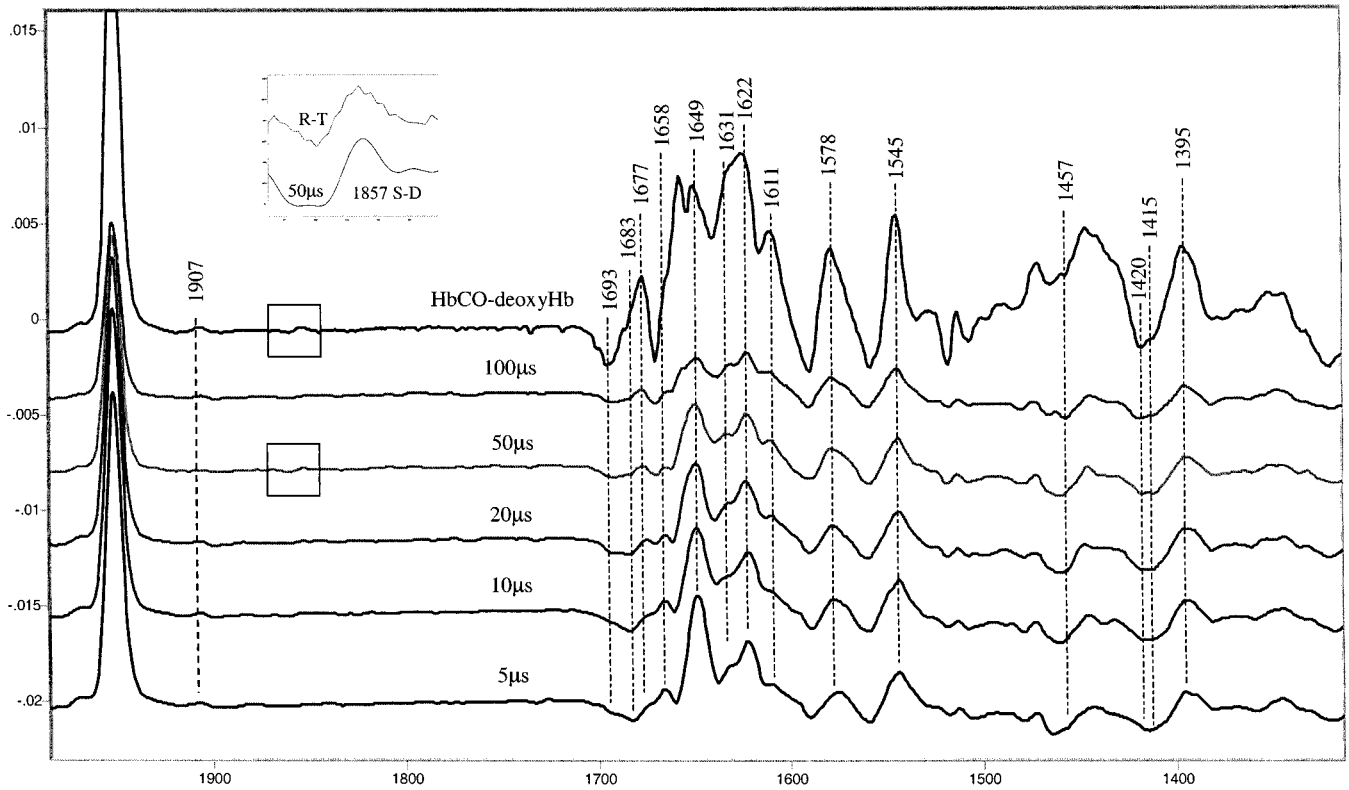

Figure 5. Difference FTIR spectra from 5 μs to 100 μs after photolysis. At the top is the static HbCO-minus-deoxyHb difference spectrum.[7]

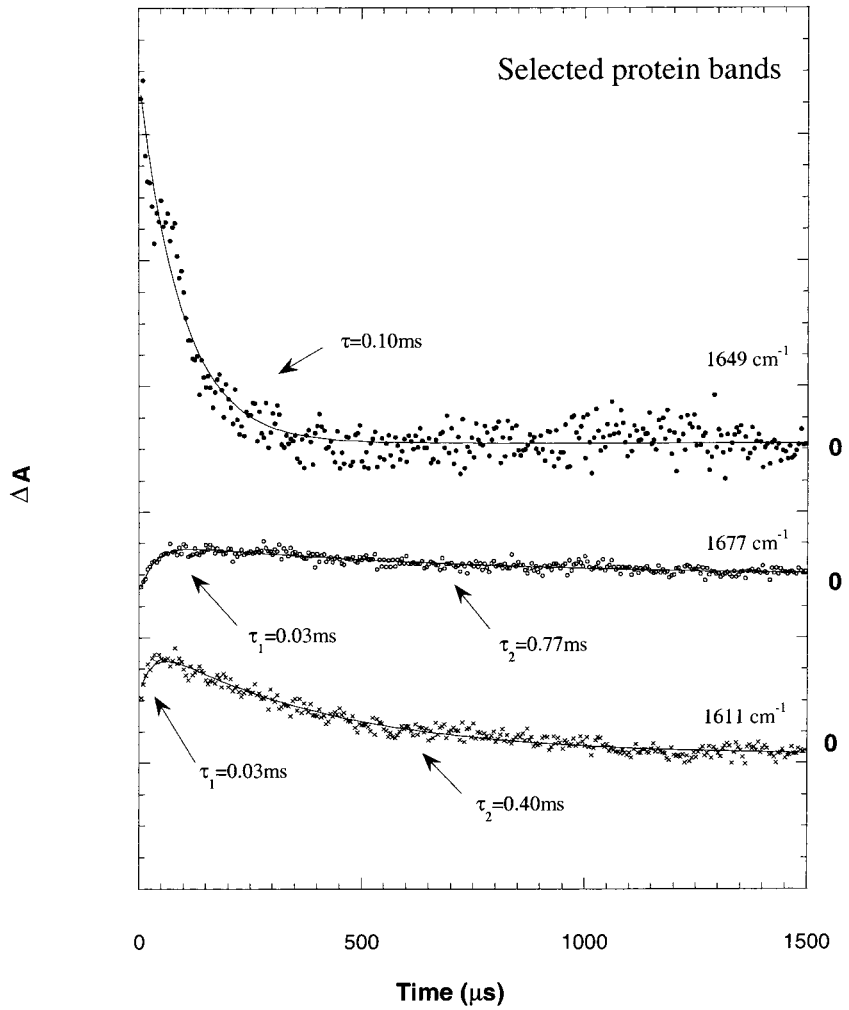

Figure 6. Evolution of the 1649, 1677, and 1611 cm^{-1} FTIR difference intensities. The time courses are fit to single (1649 cm^{-1}) or successive (1677 and 1611 cm^{-1}) exponentials, with the indicated time constants.

HbCO-minus-photoproduct difference spectra of the R and T molecules, using a single-value decomposition algorithm.[14] These spectra are shown in Figure 7 and the wavenumbers and amplitudes of the difference bands are assembled in Table 1, along with tentative assignments.

Discussion

The present work demonstrates that the R−T transition in Hb can be driven by HbCO photolysis and monitored by step-scan FTIR spectroscopy. The most direct evidence is the appearance of the 1857 cm^{-1} bisignate cysteine band, which is characteristic of the T state and appears in late but not in early microsecond spectra. This band was not seen by Hu et al.,[5] because the extent of photolysis in the early studies was too low to support T state formation.

The time course of CO rebinding to the heme can be accurately monitored via the intense stretching band of the bound CO at 1951 cm^{-1}. Geminate rebinding occurs with a yield of 50%, most of it in a 70 ns phase, in good agreement with previous results from absorption[1] and UVRR[2] transients. This phase coincides with the first protein structure change in the relaxation from the R to the T state.[1,2] The UVRR transients associated with this change indicate the breaking of H-bonds involving tryptophan and tyrosine residues as a result of displacements of the proximal (F) and distal (E) helices surrounding the heme.[2] It was suggested[3] that a rotation of the EF "clamshell" (which has actually been demonstrated in a comparison of high-resolution crystal structures of myoglobin and its CO adduct[15]) is driven by displacement of the Fe atom toward the proximal side of the heme upon deligation, and that this rotation impels the photodissociated CO either to recombine or to exit the heme pocket. The UVRR spectrum of this first

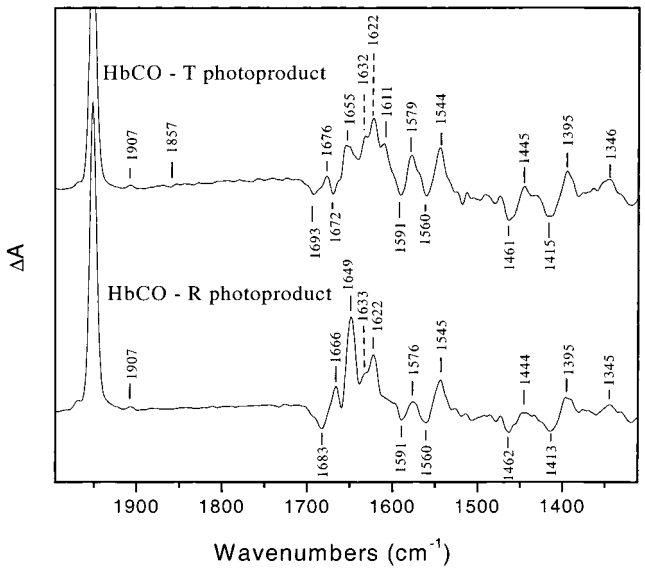

Figure 7. Computed HbCO-minus-photoproduct difference spectra for R and T state molecules, using single-value decomposition and the kinetic scheme described in the text.

protein intermediate, labeled R_{deoxy}, is mimicked by other Hb constructs that remain in the R quaternary structure but have one or more deligated subunits.[2]

The 1951 cm^{-1} FTIR band reveals an additional small (13%) fraction of geminate rebinding with a 10-fold slower rate ($\tau =$ 890 ns), which has not previously been reported, perhaps because of its low amplitude. Absorption spectroscopy did yield a kinetic phase with this time constant, but it was attributed to a second tertiary structure change of the protein.[1] This change was corroborated by UVRR spectroscopy, which established an $\sim$1 μs process involving tyrosine and tryptophan residues.[2] This process was interpreted in terms of a second protein intermediate, labeled S, whose spectrum indicated reestablishment of the H-bonds broken in the R_{deoxy} structure. It was suggested[3] that this process involves motions of the outer helices, A and H, which reposition the N and C termini for subsequent formation of the anchoring salt-bridges that characterize the T quaternary structure.[16] We suggest that the R_{deoxy}-to-S structure change induces recombination of CO molecules that have escaped the heme pocket but remain at other sites in the molecule, thereby accounting for the low-amplitude slow geminate phase.

The 1951 cm^{-1} band decays to zero on the microsecond time scale, due to rebinding of CO from the solution. This decay has a fast and a slow component, as also seen in absorption transients[1] and as is expected from the different rates associated with the R and T quaternary structures.[11,12] Although these are second-order processes, the system is too complex to support fitting the experimental time course to second-order kinetics. Two successive exponentials are adequate to fit the data to within experimental error [Figure 4], and the time constants, 80 and 670 μs, are in reasonable accord with what would be expected on the basis of the reported second-order rate constants.[12]

These time constants are also in accord with the behavior of the FTIR difference bands associated with the protein residues [Figure 6]. One of them, at 1649 cm^{-1}, decays with a 100 μs time constant, indicating that it arises almost entirely from molecules in the R quaternary structure. Another, at 1677 cm^{-1}, decays with a 770 μs time constant, indicating that it arises from molecules in the T quaternary structure. However, it also displays an initial rise, with a 30 μs time constant. This value is associated with the R to T quaternary transition; it is close to the $\sim$20 μs value expected on the basis of absorption[1] and UVRR[2] transients. Most of the protein difference FTIR bands have mixed behavior, with a 30 μs rise followed by decay, with time constants between 100 and 770 μs, indicating contributions from molecules in both quaternary states.

The evolution from R to T state molecules can be seen qualitatively in the FTIR difference spectra recorded during the first 100 μs [Figure 5]. On the basis of the kinetic scheme involving parallel rebinding to R (80 μs) and T state (670 μs) molecules, with rapid (30 μs) R$-$T relaxation, we computed the time course of the species concentrations and extracted the difference FTIR spectra of molecules in the R and T quaternary structures, using singular value decomposition [Figure 7]. Because of the averaging over many time slices, these spectra are of high quality, as can be seen in the well-resolved 1907 cm^{-1} band, which is the ^{13}CO (1.08% natural abundance) satellite of the 1951 cm^{-1} band. The 1857 cm^{-1} bisignate band appears in the computed difference spectrum for T but not for R state molecules, as expected.

Most of the difference bands are at the same positions for R and T molecules, differing only modestly in amplitude [Table 1]. We infer that these bands result from tertiary changes associated with the loss of CO molecules from the tetramers. It seems likely that changes common to both quaternary structures are more or less localized to the residues on the E and F helices, which are the most likely to be perturbed by loss of a ligand. Identification of specific residues will require isotope labeling and/or site mutants. Table 1 offers suggestions for generic assignments. For example, the bands at 1396 and 1578 cm^{-1} are at positions expected for the symmetric and asymmetric stretches of carboxylate side chains. Several Asp and Glu residues reside on the E and F helices.

There are, however, difference bands that are strikingly different for photoproduct molecules in the R vs the T state. The most prominent of these are the 1649 and 1683 cm^{-1} R state bands, which are essentially absent in the T molecules. The 1649 cm^{-1} position is characteristic for the amide I vibration of α-helical peptide groups,[18] while the much higher 1683 cm^{-1} position is suggestive of an amide carbonyl group which is not H-bonded. The 1649 cm^{-1} intensity is higher in HbCO while the 1683 cm^{-1} intensity is higher in the photoproduct, suggesting that one or more α-helical peptide carbonyls lose their H-bond in the photoproduct. (The larger amplitude for the 1649 cm^{-1} than for the 1683 cm^{-1} band is consistent with the expected increase in absorbance upon H-bonding.)

We offer the suggestion that these carbonyls might belong to a pair of valine residues, α93 and β95. In both deoxyHb and HbCO these F-helix residues accept H-bonds from tyrosine OH groups on the H-helix residues α140 and β145.[16] These are among the interhelical H-bonds that are proposed to break in the R_{deoxy} intermediate and reform in the S intermediate.[3] Very recent UVRR measurements indicate that the interhelical H-bonds do not reform synchronously, but that the tyrosine H-bonds lag behind the tryptophan H-bonds.[17] The time constant for reformation of the tyrosine H-bonds is about 5 μs.

Thus the apparent shift in carbonyl frequency from 1649 to 1683 cm^{-1} could be understood if the R photoproduct represents an intermediate structure of the protein in which the Val α93 and β95 H-bonds have not yet reformed. This would be consistent with the first time slice in the microsecond regime of the FTIR measurements being 5 μs. We note that the intensity of the 1622 cm^{-1} difference band may support this interpretation. This positive band is about 60% stronger in the R than in the T state, possibly as a consequence of the absence of the Tyr$-$Val H-bonds. The frequency is close to the expected position of the tyrosine Y8a mode,[2] whose intensity should increase when the OH group donates an H-bond, as the Tyr α140 and β145 residues do in HbCO and in the T photoproduct. (There are four additional Tyr residues, which can contribute to this band, possibly accounting for the intensity difference between HbCO and the T photoproduct.)

There are also bands that are unique to the T photoproduct: positive bands at 1611 and 1655 cm^{-1} and negative bands at 1672 and 1693 cm^{-1}. These are also seen in the static HbCO-minus-deoxyHb difference spectrum [Figure 5]. No structural interpretation is immediately obvious. The 1693 cm^{-1} band had been thought to reflect protonation of an aspartate residue in the T state,[7] but this was subsequently disproved by isotope labeling.[19]

Conclusion

Step-scan infrared spectroscopy is shown to be capable of monitoring the allosteric transition in Hb, using saturating photolysis conditions. The strong 1951 cm^{-1} CO band provides a sensitive monitor of CO rebinding and has permitted discovery

of a slow (890 ns) geminate phase. This phase is suggested to be driven by the second tertiary protein transition (R_{deoxy} to S) and to involve CO molecules that have escaped the heme pocket and reside elsewhere in the molecule. Difference FTIR bands associated with protein vibrations show a clear-cut evolution from the R to the T photoproduct on the microsecond time scale. The most interesting signals are a pair of R photoproduct bands that may result from the breaking and reforming of Tyr−Val interhelical H-bonds at intermediate stages of the allosteric transition.

Acknowledgment. This work was supported by NIH grant GM 25158 from the National Institute of General Medical Sciences. We thank Dr. Andrzej Jarzecki for help with the computations.

References and Notes

(1) Hofrichter, J.; Sommer, J. H.; Henry, E. R.; Eaton, W. A. *Proc. Natl. Acad. Sci. U.S.A.* **1983**, *80*, 2235. (b) Henry, E. R.; Jones, C. M.; Hofrichter, J.; Eaton, W. A. *Biochemistry* **1997**, *36*, 6511.

(2) Jayaraman, V.; Rodgers, K. R.; Mukerji, I.; Spiro, T. G. *Science* **1995**, *269*, 1843.

(3) Hu, X.; Rodgers, K. R.; Mukerji, I.; Spiro, T. G. *Biochemistry* **1999**, *38*, 3462.

(4) Weidlich, O.; Siebert, F. *Appl. Spectrosc.* **1993**, *47*, 1394. (b) Gerwert, K.; Hess, B.; Soppa, J.; Oesterhelt, D. *Proc. Natl. Acad. Sci. U.S.A.* **1989**, *86*, 4943. (c) Hage, W.; Kim, M.; Frei, H.; Mathies, R. A. *J. Phys. Chem.* **1996**, *100*, 16026.

(5) Hu, X.; Frei, H.; Spiro, T. G. *Biochemistry* **1996**, *35*, 13001.

(6) Antonini, E.; Brunori, M. In *Hemoglobin and Myoglobin and their Reactions with Ligands;* Neuberger, A., Tatum, E. L., Eds.; Elsevier: New York, 1971; pp 2−4.

(7) Gregoriou, V. G.; Jayaraman, V.; Hu, X.; Spiro, T. G. *Biochemistry* **1995**, *34*, 6876.

(8) Uhmann, W.; Becker, A.; Taran, C.; Siebert, F. *Appl. Spectrosc.* **1991**, *45*, 390.

(9) Ansari, A.; Jones, C. M.; Henry, E. R.; Hofrichter, J.; Eaton, W. A. *Biophys. J.* **1993**, *64*, 852.

(10) Jones, C. M.; Ansari, A.; Henry, E. R.; Christoph, G. W.; Hofrichter, J.; Eaton, W. A. *Biochemistry* **1992**, *31*, 6692.

(11) Gibson, Q. H. *Biochem. J.* **1959**, *71*, 293. (b) Sawicki, C.; Gibson, Q. H. *J. Biol. Chem.* **1976**, *251*, 1533.

(12) Mathews, A. J.; Olson, J. S. *Methods Enzymol.* **1994**, *232*, 363.

(13) Alben, J. O.; Bare, G. H. *J. Biol. Chem.* **1980**, *255*, 3892.

(14) Henry, E. R.; Hofrichter, J. *Methods Enzymol.* **1992**, *210*, 129.

(15) Kachalova, G. S.; Popov, A. N.; Bartunik, H. D. *Science* **1999**, *284*, 473.

(16) Perutz, M. F.; Wilkinson, A. J.; Paoli, M.; Dodson, G. G. *Annu. Rev. Biophys. Biomol. Struct.* **1998**, *27*, 1−34.

(17) Balakrishnan et al., in prep.

(18) Austin, J.; Jordan, T.; Spiro, T. G.; In *Advances in Infrared and Raman Spectrosocpy*; Clark, R. H. J., Hester, R. E.; Eds.; Wiley: Chichester, U.K., 1993; p 53.

(19) Hu, X.; Dick, L. A.; Spiro, T. G. *Biochemistry* **1998**, *37*, 7, 9445.